Extremum Seeking Control for optimization of a feed-forward Pelton turbine speed controller in a fixed-displacement hydraulic wind turbine concept

Mulders, S. P.; Diepeveen, N. F.B.; Van Wingerden, J. W.

DOI
10.1088/1742-6596/1222/1/012015

Publication date
2019

Document Version
Final published version

Published in
Journal of Physics: Conference Series

Extremum Seeking Control for optimization of a feed-forward Pelton turbine speed controller in a fixed-displacement hydraulic wind turbine concept

IOP Conf. Series: Journal of Physics: Conf. Series **1222** (2019) 012015 doi:10.1088/1742-6596/1222/1/012015

Extremum Seeking Control for optimization of a feed-forward Pelton turbine speed controller in a fixed-displacement hydraulic wind turbine concept

SP Mulders[1], NFB Diepeveen[2], JW van Wingerden[1]

1. Delft Center for Systems and Control, Faculty of Mechanical Engineering, Delft University of Technology, Mekelweg 2, 2628 CD Delft, The Netherlands
2. DOT B.V., Raam 180, 2611 WP Delft, The Netherlands

E-mail: s.p.mulders@tudelft.nl[1], niels@dotpower.nl[2]

Abstract. With the sustained drive towards higher power ratings for offshore wind turbines, the size of the turbine rotor and drivetrain components scale accordingly. Compact hydraulic transmissions are widely applied in high-load systems and form a business case for application in multi-megawatt offshore turbines. The Delft Offshore Turbine (DOT) is a hydraulic wind turbine concept replacing conventional drivetrain components with a single seawater pump. In the DOT concept, pressurized seawater is directed to a Pelton turbine-generator combination, located at a central electricity generation platform. An in-field test campaign is performed using a prototype DOT turbine with a retrofitted 500 kW hydraulic drivetrain, consisting of fixed-displacement components. As a result of this configuration, a feed-forward Pelton speed controller is derived and implemented for operating the Pelton turbine at maximum efficiency. However, the controller tuning is based on estimations of physical system properties, of which the resulting optimality is unknown. For verification of the implementation, the model-free, gradient-based and data-driven Extremum Seeking Control (ESC) optimization scheme is employed. Results show fast convergence of the algorithm and an average maximum power increase of 3 %. The algorithm is well suited for application to real-world systems, due to its simplicity and ease of tuning.

1. Introduction

While the conventional drivetrain of a horizontal-axis wind turbine (HAWT) is a proven concept, the weight contribution of all components in the nacelle results in a rather high total mass. The complete turbine support structure is designed to carry this weight for the entire expected lifetime, which in turn leads to extra material and thus total cost of the wind turbine [1]. In an effort to reduce turbine maintenance requirements, complexity, weight and thus the Levelized Cost of Energy (LCOE) for offshore wind, a novel and patented [2] hydraulic concept is proposed by Delft Offshore Turbine (DOT). The eponymous turbine only requires a single water pump directly connected to the turbine rotor and replaces high-maintenance components in the nacelle, which is in effect favorable for all aforementioned aspects. In contrast to conventional wind farms, DOTs are designed to operate in a hydraulic network of multiple turbines, collectively pressurizing seawater to a central multi-megawatt generator platform. At this central location, the hydrodynamic energy is converted to electrical energy. A study on the design of the hydraulic

DOT drivetrain is performed in [3], whereas the feasibility of multiple turbines in a hydraulic network has been investigated in [4].

In 2016, extensive prototype tests have been performed with an in-field, full-scale and retrofitted wind turbine, of which the conventional drivetrain is replaced by a 500 kW hydraulic configuration [5]. The DOT500 prototype, shown schematically and physically in Figure 1, includes an intermediate oil loop providing a *hydraulic gearbox* between the low-speed oil pump directly connected to the rotor, and the high-speed water pump at the tower bottom. The pressurized water flow is converted to a high-speed water jet by means of a spear valve. The jet is then directed to a Pelton turbine wheel mechanically coupled to an asynchronous generator.

Figure 2 shows a visualization of the employed Pelton-spear valve set-up. Because all drivetrain components have a fixed volumetric displacement (apart from volumetric losses), the system pressure varies according to the turbine operating conditions. Consequently, the speed of the Pelton wheel needs to be controlled by the generator to maximize its efficiency at each operating point. As the feed-forward speed controller is derived from physical relations and its tuning is based on an estimation of system properties, the implementation might not be optimal in practice.

Extremum Seeking Control (ESC) is employed for optimization of the feed-forward controller. Results show the effectiveness of the ESC implementation for optimization of the controller on the real-world test set-up. The feed-forward gain is reduced by 13.5 % leading to a power increase of 3 %. The explanation for the rather large discrepancy between the theoretical and optimized gain later appeared to be caused by an erroneous pressure sensor reading, however, the application of ESC led to the discovery of the error.

This paper is organized as follows. Section 2 presents the principles of optimal Pelton turbine operation using a feed-forward control strategy, and subsequently elaborates on the ESC implementation for controller optimization. Section 3 presents the optimization and power extraction results obtained from the in-field prototype DOT500 wind turbine. A combined section with conclusions and a discussion on learning objectives is given by Section 4.

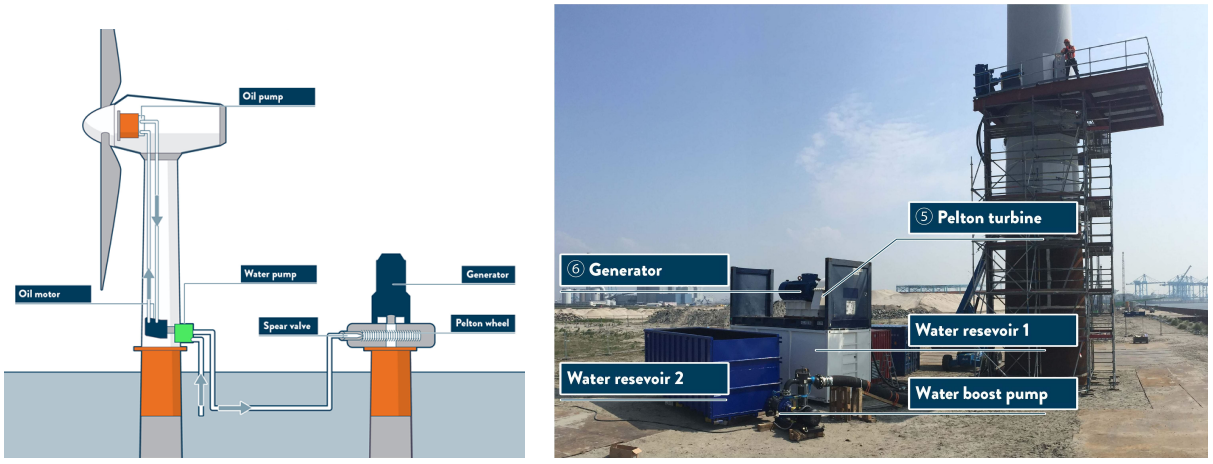

(a) (b)

Figure 1: A schematic figure (a) of the prototype DOT500 set-up with intermediate oil loop acting as a *hydraulic gearbox* between the oil pump and water pump. The photograph (b) shows the in-field test set-up where the combined generator-Pelton turbine configuration is located at ground level.

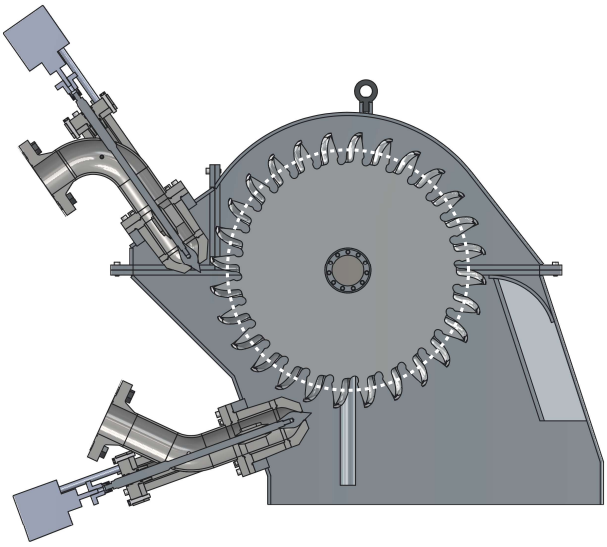

Figure 2: A Pelton wheel driven by the high-velocity water jets from two spear valves with controllable nozzle area for pressure control. The dashed circle indicates the pitch circle diameter.

2. Approach

This section is divided in two subsections. In Section 2.1, the general principles of optimal Pelton turbine operation are outlined using physical first-principles hydraulic relations. The result is used for derivation of a feed-forward speed control strategy. In Section 2.2, the ESC algorithm is described and the implementation for online optimization of the feed-forward gain is outlined.

2.1. Pelton turbine efficiency analysis and derivation of a feed-forward speed controller

Most Pelton turbines are operated under constant head pressure conditions, allowing for connection to a synchronous electrical generator. Recent works on the design of hydraulic wind turbines focus on a constant pressure discharge water flow. This is accomplished by combined controller implementations on the pump variable volumetric displacement and control of spear valves with variable effective orifice areas [4, 15, 16]. This allows the Pelton turbine to operate at its optimal fixed-speed efficiency point, and the application of a synchronous generator.

As a consequence of the DOT500 drivetrain design with fixed-displacement components, the pump discharge pressure needs to be controlled for providing for region 2 torque control substitute [5]. Resulting from this varying line pressure, the outgoing hydrodynamic water jet mass flow and velocity varies. To ensure optimal Pelton efficiency, a fixed ratio between the Pelton tangential speed and the incoming water jet speed needs to be maintained [17]. The asynchronous generator – mechanically coupled to the Pelton wheel – is supplied with the speed set point calculated by a feed-forward speed controller. The remainder of this section is devoted to the derivation of this controller.

The high-pressure water flow is converted to a high-velocity water jet. Both quantities are related by Bernoulli equation [18] for incompressible flows

$$v_\mathrm{j} = \sqrt{v_\mathrm{w}^2 + \frac{2(p_\mathrm{w} - p_\mathrm{j})}{\rho_\mathrm{w}}} \approx \sqrt{\frac{2p_\mathrm{w}}{\rho_\mathrm{w}}}, \tag{1}$$

in which v_j and p_j are respectively the speed and pressure of the water jet exiting the spear valve, v_w and p_w the speed and pressure of the in-line water flow, and the density of water ρ_w is taken constant. The approximation in Equation (1) is based on the assumption that the jet has

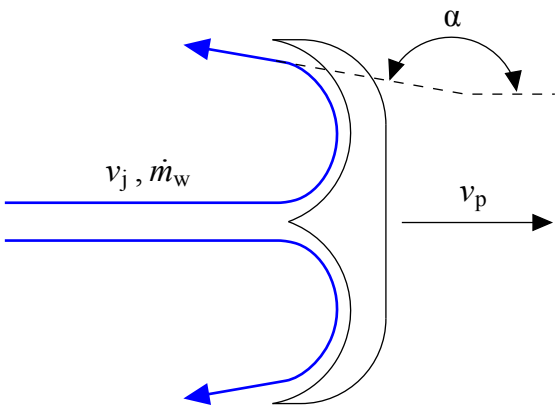

Figure 3: Schematic showing the relation between the incoming water jet speed v_j, the tangential bucket speed v_p, and their relative speed v_r.

an atmospheric pressure $p_j = p_0$, and the squared speed of the in-line water flow is negligible with respect to the second term in the square root. The tangential bucket speed of the Pelton turbine v_p is related to the rotational free-run speed ω_p of the turbine by

$$v_p = \omega_p \frac{D_p}{2}, \tag{2}$$

where D_p is the turbine pitch circle diameter (PCD), indicated by the dashed circle in Figure 2. From this, the relative velocity between the water and bucket speed is given by

$$v_r = v_j - v_p, \tag{3}$$

where it is assumed that the water speed is maintained in the bucket [17]. The momentum of the high-speed water jet exerts a force on the moving Pelton buckets

$$F_p = \rho_w Q_w v_r (1 - \cos\alpha) = \dot{m}_w v_r (1 - \cos\alpha), \tag{4}$$

in which α is the angle between bucket incoming and outgoing water flow shown in Figure 3, Q_w is the water volumetric flow rate, and $\dot{m}_w$ the water mass flow rate. The efficiency of the Pelton turbine is expressed as the ratio between the mechanical power available at the Pelton shaft and the kinetic power contained in the water jet: $\eta_p = P_p/P_w$. The kinetic power of the water jet is given by

$$P_w = \frac{1}{2}\dot{m}_w v_j^2, \tag{5}$$

and the mechanical Pelton power is defined as

$$P_p = F_p v_p = \dot{m}_w v_r (1 - \cos\alpha) v_p. \tag{6}$$

Now by rewriting the Pelton efficiency equation, and defining the ratio between the Pelton bucket and water jet speed as $\kappa_v = v_p/v_j$, the following expression is obtained

$$\eta_p = 2\kappa_v (1 - \kappa_v)(1 - \cos\alpha). \tag{7}$$

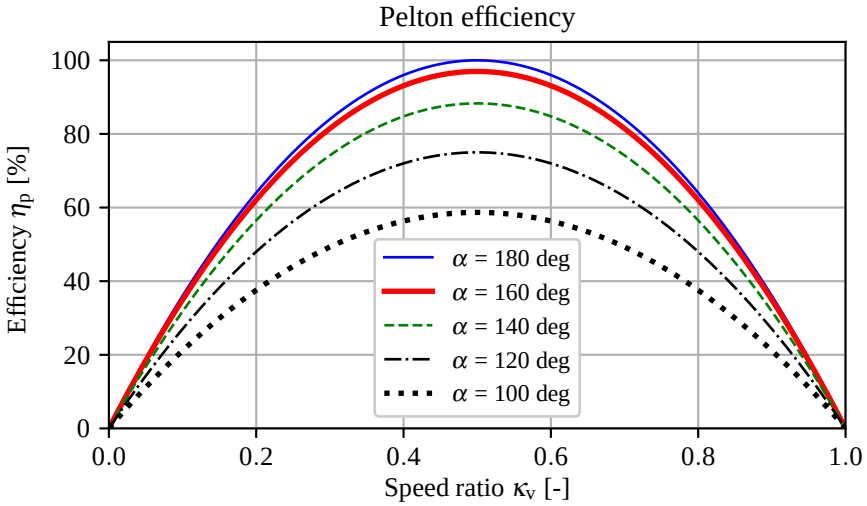

Figure 4: Pelton efficiency η_p as function of the ratio between the bucket speed and water jet. The efficiency is evaluated for multiple deflection angles α.

Solving the efficiency gradient for $\partial\eta_p/\partial\kappa_v = 0$, gives the ratio $\kappa_v = 1/2$ for maximum Pelton efficiency. An evaluation of this relation for different deflection angles α is visualized in Figure 4, and it is observed that the optimal ratio κ_v is independent of α.

As it is now known that for maximum efficiency the water jet velocity should be twice the tangential bucket speed ($v_j = 2v_p$), a feed-forward generator speed controller is derived. By this information, and substitution of Equations (1) and (2), the feed-forward generator speed controller is defined as

$$\omega_g = \sqrt{\frac{2p_w}{\rho_w D_p^2}} = K_{FF}\sqrt{p_w}. \tag{8}$$

All non-varying parameters are captured in a single constant K_{FF}, and the water pressure p_w is a measured quantity.

Remark 1 *After the water flow exits the spear valve, the aim to operate the Pelton turbine-generator combination at maximum efficiency is a decoupled control objective from the rest of the wind turbine drivetrain. This paper only considers the optimization of the Pelton-generator system. As the control of this system does not influence the wind turbine operating behavior, the relation to the extracted wind turbine energy/power is omitted. For an extensive description of the wind turbine drivetrain and its controller design, the reader is referred to [5].*

2.2. Theory on Extremum Seeking Control

The online, model-free and gradient-based optimization scheme Extremum Seeking Control (ESC) [6, 7] is applicable to parameters in a (control) system, of which the optimization objective function possesses a local optimum. The first notion of ESC is found in [8], whereas the algorithm was for the first time described in detail in the 1950's [9]. ESC has seen a revival at the beginning of the current century with a proof of stability [10]. At present, the algorithm is of great interest [7], with the trend of increasingly complex systems and the scheme's ease of implementation. ESC has shown being effective in optimizing the region 2 torque control gain of a conventional wind turbine [11, 12], but also for control optimization of multiple turbines in a wind farm setting [13, 14].

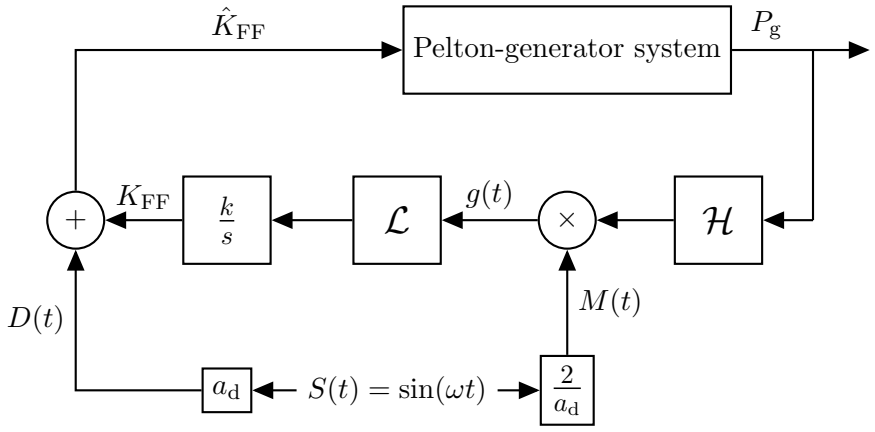

Figure 5: Block diagram of ESC implemented on the Pelton-generator system. The feed-forward gain K_{FF} is excited by the dither signal $D(t)$, and $M(t)$ is used for demodulation of the high-pass filtered generator power output signal P_{g}. After demodulation, the gradient information of $\partial P_{\mathrm{g}}/\partial K_{\mathrm{FF}}$ is contained as a DC-contribution in $g(t)$, which is subsequently low-pass filtered and integrated to arrive at the optimal value for K_{FF}.

Substitution of the physical system properties included in K_{FF} (Equation (8)) leads to the definition of a feed-forward Pelton turbine control implementation. By tracking the calculated speed set point ω_{g} results in Pelton operation at maximum efficiency for each operating pressure. However, due to inevitable discrepancies between theory and practice, the non-varying constant K_{FF} might not be optimal on the real-world set-up. For this reason, the model-free and data-driven ESC optimization algorithm is implemented.

Figure 5 presents a schematic of the continuous-time ESC implementation. The scheme aims for maximization of the generator power P_{g}, provided by an instantaneous sensor reading. The ESC algorithm is based on a dither-demodulation scheme by periodic excitation of K_{FF}, taken as the input of the plant

$$\hat{K}_{\mathrm{FF}} = K_{\mathrm{FF}} + D(t) = K_{\mathrm{FF}} + a_{\mathrm{d}} \sin(\omega t). \tag{9}$$

The dither and demodulation signals $D(t)$ and $M(t)$, respectively, are amplitude-scaled versions of the periodic excitation signal $S(t)$. By exciting the system input with the dither signal, and multiplying the generator power output P_{g} with the demodulation signal, gradient information is present as a DC contribution in the resulting signal $g(t)$. This can be seen by rewriting the system output signal as a first-order Taylor series expansion

$$P_{\mathrm{g}}(\hat{K}_{\mathrm{FF}}) = P_{\mathrm{g}}(K_{\mathrm{FF}} + a\sin(\omega t)) \approx P_{\mathrm{g}}(K_{\mathrm{FF}}) + a\sin(\omega t)\frac{\partial P_{\mathrm{g}}}{\partial \hat{K}_{\mathrm{FF}}} + \mathcal{O}^2. \tag{10}$$

The high-pass filter $\mathcal{H}$ removes the steady-state component, and by subsequent multiplication with $M(t)$ and by rewriting using trigonometric identities, one obtains

$$2\sin^2(\omega t)\frac{\partial P_{\mathrm{g}}}{\partial \hat{K}_{\mathrm{FF}}} = \frac{\partial P_{\mathrm{g}}}{\partial \hat{K}_{\mathrm{FF}}} - \cos(2\omega t)\frac{\partial P_{\mathrm{g}}}{\partial \hat{K}_{\mathrm{FF}}}. \tag{11}$$

The algorithm converges to a *steady-state* value of K_{FF} such that output P_{g} is optimized and the gradient $\partial P_{\mathrm{g}}/\partial \hat{K}_{\mathrm{FF}}$ converges to zero. As a result of phase losses in the system, the phase of the demodulation signal can be compensated to match the phase of the output excitation signal,

resulting in improved convergence of the algorithm [11]. The integrator gain k determines the convergence rate of the algorithm, and is a trade-off between convergence speed and stability. Furthermore, the excitation frequency ω should be chosen within the bandwidth of the system input-output dynamics. For a description of tuning the low- and high-pass filter cut-off and cut-in frequencies ω_l and ω_h, the reader is referred to [6, 11].

3. Main body

The goal of this section is to verify the optimality of the theoretically determined feed-forward gain using the ESC framework described in Section 2. The theoretical values defining the gain are respectively the water density and the PCD, $\rho_\mathrm{w} = 1025\ \mathrm{kg\,m^{-3}}$ and $D_\mathrm{p} = 0.85$ m, and evaluation leads to $K_\mathrm{FF} = 5.2 \cdot 10^{-2}\ (\mathrm{rad\,s^{-1}})\,\mathrm{Pa^{-1/2}}$. The objective of the ESC scheme is maximization of the electrical power supplied by the generator

$$K^*_\mathrm{FF} = \arg\max_{K_\mathrm{FF}} P_\mathrm{g}(\hat{K}_\mathrm{FF}). \tag{12}$$

The frequency of the excitation signal $S(t)$ is chosen as $\omega = 0.04\ \mathrm{rad\,s^{-1}}$, which is well within the system bandwidth from generator speed to measured power. The low- and high-pass filters are configured to have their cut-off and cut-in frequencies at $\omega_\mathrm{l} = 0.0230\ \mathrm{rad\,s^{-1}}$ and $\omega_\mathrm{h} = 0.0205\ \mathrm{rad\,s^{-1}}$. The dither amplitude is set $a_\mathrm{d} = 3 \cdot 10^{-3}$ to allow for a peak-to-peak generator speed variation of approximately 10 %. The integrator gain is set to $k = 1 \cdot 10^{-3}$, and is found empirically to provide a satisfactory trade-off between algorithm convergence speed and stability.

The performed ESC optimization experiment, of which the results are shown in Figure 6, has a duration of approximately 1 hour. The initial condition of the integrator is set to the theoretical optimal feed-forward gain of $K_\mathrm{FF,0} = 5.2 \cdot 10^{-2}\ (\mathrm{rad\,s^{-1}})\,\mathrm{Pa^{-1/2}}$. Convergence of the algorithm is observed in the first half of the experiment, after which the algorithm converges to an optimal gain of $K^*_\mathrm{FF} = 4.5 \cdot 10^{-2}\ (\mathrm{rad\,s^{-1}})\,\mathrm{Pa^{-1/2}}$. The obtained result is a decrease of 13.5 %, and shows a significant deviation from the theoretically derived result.

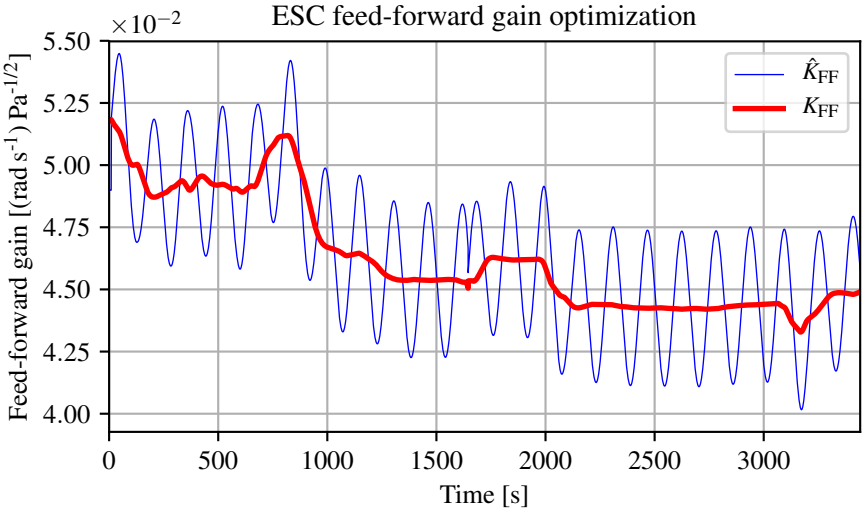

Figure 6: ESC optimization progress of the feed-forward generator speed controller gain K_FF. Convergence to a lower value is observed during the first 2000 s, while this value remains near constant in the second half of the process.

To verify whether the optimized controller gain indeed results in a higher efficiency of the Pelton turbine-generator system, two 10 minute verification data sets are performed: one with the theoretical, and the other with the optimized gain. The results are presented in Figure 7. Figure 7a illustrates the generator speed difference for the two cases, and shows a significant drop of the operational generator speed. Figure 7b evaluates the generated power for the same experiment. Because limited verification data is available, no profound statement can be made on the overall performance. However, it is possible to evaluate the average maximum power, which is defined as all the data points that are above a boundary value of 90 kW. It is observed that the average maximum power is higher for the case using the optimized controller gain. An average maximum power of 100 kW and 103 kW is obtained for the respective cases.

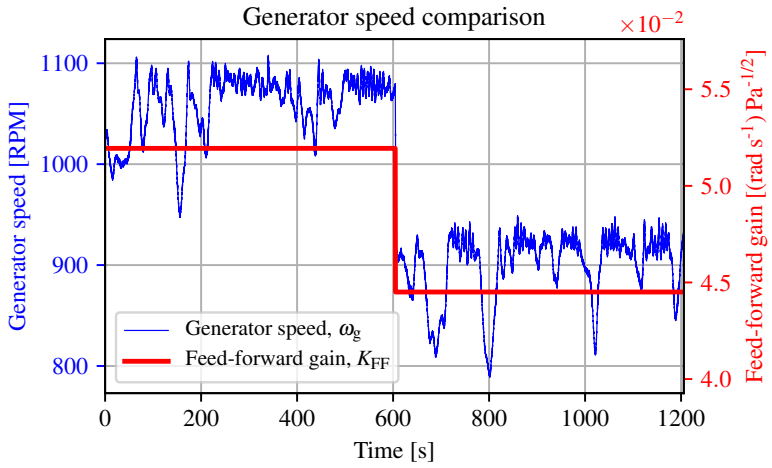

(a)

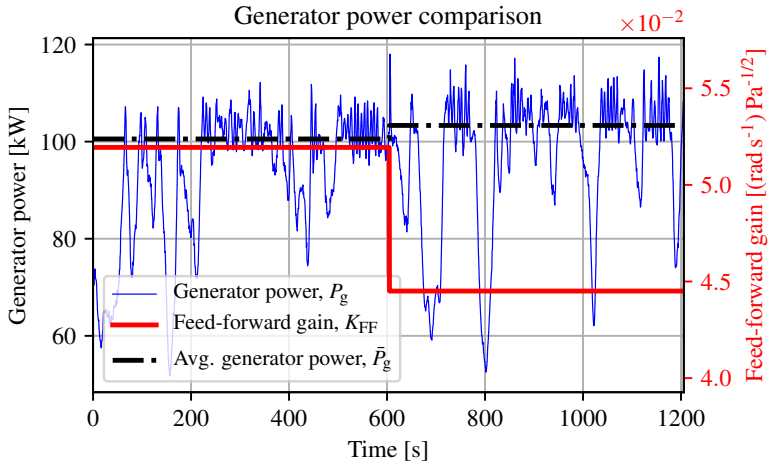

(b)

Figure 7: The effect of implementing the the theoretical and optimized gain on generator speed (a) and generated power (b). In the latter plot, an average maximum power of 100 kW and 103 kW is found for the respective cases.

4. Conclusions and learning objectives

This paper shows the implementation of a feed-forward speed controller for operating a Pelton turbine at its maximum efficiency under varying conditions. A theoretical estimation of the feed-forward gain can be derived from physical relations, however, the optimality on a practical real-world system is unknown. For verification, the model-free, gradient-based and data-driven optimization scheme Extremum Seeking Control is employed on the feed-forward gain on the practical test set-up. The algorithm shows fast convergence and a decrease of 13.5 % of the feed-forward gain, resulting in an average maximum power increase of 3 %. The explanation for the rather large discrepancy between the theoretical and optimized gain later appeared to be related to an error in the measured pressure value, however, the application of ESC led to the discovery of this error. It is concluded that ESC is a valuable algorithm for parameter validation and optimization. The algorithm is well suited for application to real-world systems, due to its simplicity and ease of tuning.

References

[1] Morthorst P E and Awerbuch S 2009 *The economics of wind energy* (European Wind Energy Association (EWEA))
[2] van der Tempel J 2009 Energy extraction system, has water pump attached to rotor, windmill for pumping water from sea, water system connected to water pump, for passing water pumped from sea, and generator connected to water system
[3] Diepeveen N 2013 *On the application of fluid power transmission in offshore wind turbines* Ph.D. thesis Delft University of Technology
[4] Jarquin Laguna A 2017 *Centralized electricity generation in offshore wind farms using hydraulic networks* Ph.D. thesis Delft University of Technology
[5] Mulders S P, Diepeveen N F B and van Wingerden J W 2018 *Wind Energy Science* **3** 615–638
[6] Ariyur K B and Krstic M 2003 *Real-time optimization by extremum-seeking control* (John Wiley & Sons)
[7] Tan Y, Moase W H, Manzie C, Nešić D and Mareels I M Y 2010 *29th Chinese Control Conference (CCC)*
[8] Leblanc M 1922 *Revue Generale de lElectricite*
[9] Draper C S and Li Y T 1951 *Principles of optimalizing control systems and an application to the internal combustion engine* (American Society of Mechanical Engineers)
[10] Krstić M and Wang H H 2000 *Automatica* **36** 595–601
[11] Xiao Y, Li Y and Rotea M A 2018 *IEEE Transactions on Control Systems Technology*
[12] Rotea M A 2017 *IFAC-PapersOnLine* **50** 4504–4509
[13] Boersma S, Doekemeijer B M, Gebraad P, Fleming P A, Annoni J, Scholbrock A K, Frederik J and van Wingerden J W 2017 *Proc. of the American Control Conference (ACC)* ed Sun J and Jiang Z P (United States: IEEE) pp 1–18 ISBN 978-1-5090-4583-9
[14] Ciri U, Rotea M A and Leonardi S 2017 *Renewable Energy* **113** 1033–1045
[15] Skaare B, Hörnsten B and Nielsen F G 2013 *Wind Energy* **16** 1259–1276
[16] Buhagiar D, Sant T and Bugeja M 2016 *Journal of Dynamic Systems, Measurement, and Control* **138** 081007
[17] Zhang Z 2007 *Proceedings of the Institution of Mechanical Engineers, Part A: Journal of Power and Energy* **221** 343–355
[18] White F M 2011 *Fluid Mechanics* 7th ed (McGraw-Hill)